JOURNAL OF MATERIALS SCIENCE **40** (2005) 1517–1519 LETTERS

Preparation of colloidal Pd nanoparticles by an ethanolamine-modified polyol process

FENGXI CHEN*, ZIYI ZHONG
Institute of Chemical and Engineering Sciences, 1 Pesek Road, Jurong Island, Singapore 627833
E-mail: chen_fengxi@ices.a-star.edu.sg

XIAO-JUN XU
Department of Materials Science and Engineering, University of Pennsylvania,
3231 Walnut Street, Philadelphia, PA 19104, USA

JIZHONG LUO
Institute of Chemical and Engineering Sciences, 1 Pesek Road, Jurong Island, Singapore 627833

Palladium has many applications in catalysis, sensors and electronics. It has been used as a central component in H_2 sensors and as a catalyst for hydrogenation, hydrodesulfurization and metal electrolysis deposition [1]. The decrease in its particle size to nanoscale range would enhance its effects in these applications due to the increased surface to volume ratio.

A polyol process has been used to prepare Pd nanoparticles in different environments. By reduction of electrophilic Pd(II) complexes intercalated in montmorillonite at 0 °C in MeOH, highly dispersed Pd nanoparticles with average diameter, D_{av}, of 2–3 nm were produced [2]. By controlled colloidal synthesis, silica-supported Pd catalysts with D_{av} of 6–9 nm were prepared at 25–80 °C from $PdCl_2$ or $Pd(OAc)_2$ in suspension of SiO_2 and ethanol–toluene mixtures [3]. By reducing $NaPdCl_4$ solution in bicontinuous cubic phase of glycerol monooleate at 20–25 °C, Pd nanoparticles were synthesized with D_{av} of 3–4 nm [4]. By reduction of $Pd(NO_3)_2$ with ethanol under refluxing in the presence of polyvinylpyrrolidone (PVP), Pd nanoparticles with D_{av} of 5–35 nm were generated [5]. External templates (e.g., montmorillonite, surfactant bicontinuous cubic phase, 1 nm-thick ethanol-enriched surface layer on silica), or stabilizers (e.g., PVP) were required to form the Pd nanoparticles in these methods.

In this work, the Pd nanoparticles are prepared from reduction of $Pd(OAc)_2$ by ethanolamine ($HOCH_2CH_2NH_2$, EA) at room temperature (r.t.). Two functions are expected with respect to the EA molecule. One is related to its hydroxy group, which serves as a reducing agent. The other is its amine group, which protects the Pd nanoparticles from undesirable growth and aggregation via chemical interaction between Pd and NH_2 (i.e., $NH_2 \rightarrow Pd$) [6]. Both functions ensure that no extra reducing agents or stabilizers are required to form the Pd nanoparticles according to our procedure.

A typical procedure to reduce $Pd(OAc)_2$ in EA is as follows: 10 ml of EA (99.9%, Aldrich, freshly opened) and 0.17 g of $Pd(OAc)_2$ (99.9+%, Aldrich) yellow powder were stirred at r.t. and 600 rpm for 3 hr, and then filtered to get a black suspension. This suspension is stable for 1–2 days. The Pd nanoparticles were separated from the suspension by centrifugation or gravity sedimentation. After carefully decanting yellowish supernatant, the black sediment (named EA-produced Pd) was washed with absolute ethanol, and air dried at r.t. for characterizations. For comparison, the same procedure was used to prepare a control sample except with ethanol as a reducing agent (named EtOH-produced Pd).

Powder X-ray diffraction (XRD) patterns were measured on siemens D5005 with Cu K_α radiation operated at 40 mA and 40 kV. TEM images were taken with a JEOL LEM-100CXII transmission electron microscope at an accelerating voltage of 100 kV. The TEM specimens were prepared by depositing one drop of fresh suspension onto the carbon-coated Cu grids and dried under ambient conditions. X-ray photoelectron spectroscopy (XPS) was performed on a VG ESCALAB MKII spectrometer using a Mg K_α X-ray source (1253.6 eV, 120 W). All binding energies (BEs) are referred to the C1s neutral carbon peak at 284.6 eV. The FTIR spectra were recorded with a Perkin–Elmer 2000 FTIR spectrometer with the spectral resolution of 4 cm^{-1}. The FTIR samples were prepared as a pellet in a KBr matrix.

Powder XRD patterns of EA-produced and EtOH-produced Pd nanoparticles are shown in Fig. 1. Both are consistent with the standard Pd XRD pattern [ICDD 87-0645] in terms of the number of reflection peaks, their positions and relative intensity. It is noteworthy that Fig. 1a shows a background with much higher noise than Fig. 1b. This may be related to the difference in their crystallinity. However, it is not convincing that using ethanol as a reducing agent instead of EA may enhance the resulting Pd crystallinity in such an obvious extent. A more reasonable explanation should be due to the difference in their crystallite size. According to the Scherrer equation,[†] the crystallite size of the

---

[†] The crystallite size was assessed using the Scherrer equation, $D_{hkl} = 0.9\lambda/B_{hkl}?\cos\theta$, where D_{hkl} is the crystallite size, λ is the incidence wavelength of X-ray radiation, B_{hkl} is the intensity breadth, θ is the diffraction angle.

[*] Author to whom all correspondence should be addressed.

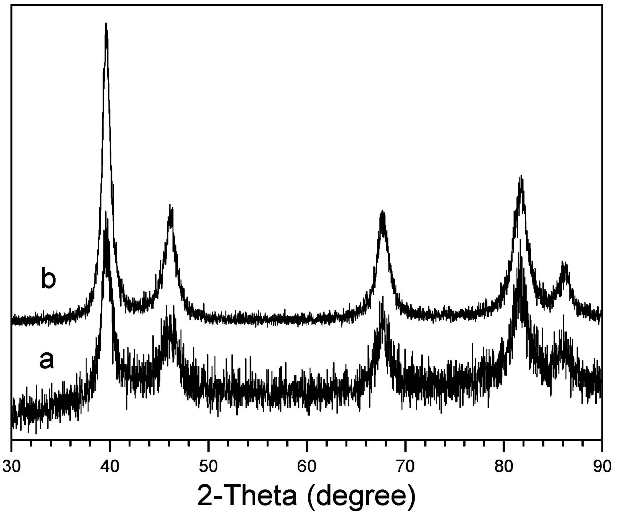

Figure 1 Powder XRD patterns for Pd nanoparticles: (a) EA-produced and (b) EtOH-produced.

EA-produced and EtOH-produced Pd nanoparticles are calculated to be 4.2 and 8.2 nm respectively.

The TEM images of the Pd nanoparticles are shown in Fig. 2. The EtOH-produced Pd nanoparticles are large aggregates (Fig. 2a), which are also reflected by their intense XRD peaks. In contrast, the EA-produced Pd nanoparticles are less agglomerated (Fig. 2b). Their average particle size was estimated from discrete particles in TEM images to be ca. 5 nm, which is very close to their crystallite size (i.e., 4.2 nm). Such small size is consistent with the expectation from their powder XRD pattern.

Chemical composition of the Pd nanoparticles is characterized by FTIR and XPS. The FTIR spectra of EA- and EtOH- produced Pd nanoparticles (Fig. 3) are quite similar. Characteristic C—H stretching modes (2923 and 2853 cm^{-1}) reveal that a hydrocarbon steric layer is adsorbed onto the particle surface. The strong adsorption at 1635 cm^{-1} indicates the presence of C=O group. The broad band at 3423 cm^{-1} can be assigned to —NH$_2$ or —OH groups. However, nitrogen signal in XPS (Fig. 4 inset) can be found only in the EA-produced Pd nanoparticles whereas it is absent in the EtOH-produced Pd. In Fig. 4, O(1s) line is obscured by the Pd(3p$_{3/2}$) core level; O KLL Auger line indicates its presence in EA- and EtOH- produced Pd [1].

TABLE I Pd$_{3d}$ binding energies and Pd^{n+}/Pd^0 atomic ratio in EA- and EtOH-produced Pd

Samples	Binding energy (eV)	Pd^{n+}/Pd^0 ratio
EA-produced Pd	Pd^0: 335.4 and 340.6 ($\Delta = 5.2$)	1
	Pd^{n+}: 336.9 and 342.0 ($\Delta = 5.1$)	0.39
EtOH-produced Pd	Pd^0: 335.1 and 340.3 ($\Delta = 5.2$)	1
	Pd^{n+}: 336.5 and 341.6 ($\Delta = 5.1$)	1.33

Pd chemical status is determined from Pd$_{3d}$ core level XPS spectra (Fig. 5). The general features of curve a and b in Fig. 5 are similar. Both are asymmetric toward high BEs, and can be deconvoluted into two sets of doublets (Table I). One set of doublet in EA-produced Pd occurs at lower BEs of 335.4 eV (3d$_{5/2}$) and 340.6 eV (3d$_{3/2}$). It is the major component of the overall profile, and can be assigned to metallic Pd [2, 7, 8]. The other set of small doublet appears at higher BEs of 336.9 eV (3d$_{5/2}$) and 342.0 eV (3d$_{3/2}$), indicating the presence of non-zerovalent Pd (Pd^{n+}) in the metallic Pd (Pd^0). The atomic ratio of Pd^{n+}/Pd^0 is obvious different between EA- and EtOH- produced Pd, i.e., 0.39 vs. 1.33. It shows that the EA-produced Pd is more resistant to be re-oxidized while handling under ambient conditions.

By comparing the two reducing systems used in this work (i.e., containing EA and EtOH respectively), amine group in EA is a key factor contributing to the differences in the particle size, morphology and chemical status of the resulting Pd nanoparticles. It provides *in-situ* protection of Pd(0) nuclei, which are generated from slow reduction of Pd(OAc)$_2$ by hydroxy group in EA.

Two other observations support the bi-function of the EA molecule, i.e., as a reducing agent and a stabilizer. Firstly, when EA or its aqueous solution (1:5 by volume of EA to water) were added into Pd(OAc)$_2$ yellow solution in toluene, a two-phase mixture was obtained. The upper toluene layer becomes colorless while the lower EA layer changes to pale yellow. After removal of the upper toluene solution, the EA solution is stable under ambient conditions for at least 2 months. This experiment shows the extraction effect of EA due to NH$_2 \rightarrow$ Pd interaction. Secondly, when Pd(OAc)$_2$ powder was stirred in EA aqueous solution (1:5 by volume of EA to water), a slightly yellow solution was obtained within 5 min. Except fewer black

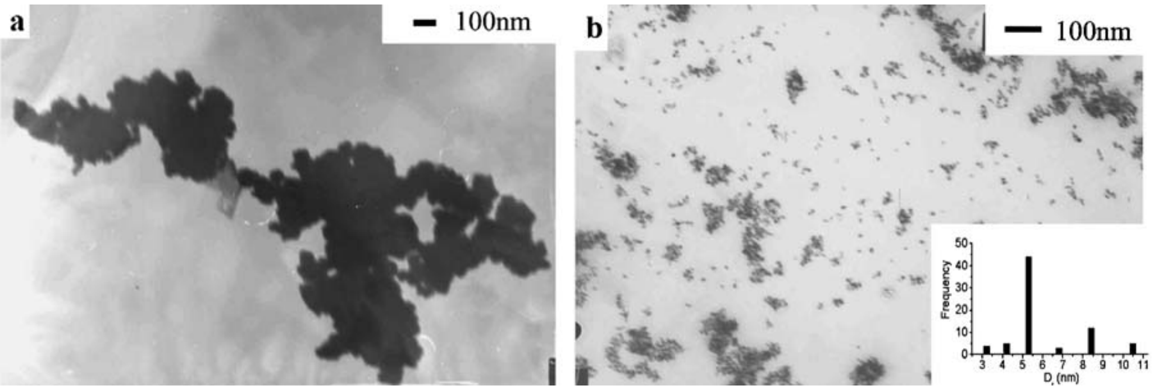

Figure 2 TEM images of Pd nanoparticles: (a) EtOH-produced and (b) EA-produced. Inset is particle size distribution.

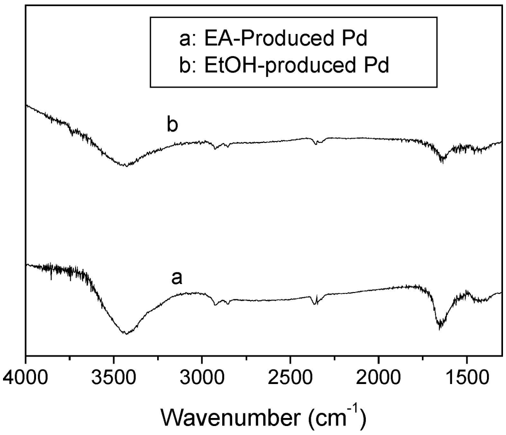

Figure 3 FTIR spectra of: (a) EA-produced Pd and (b) EtOH-produced Pd.

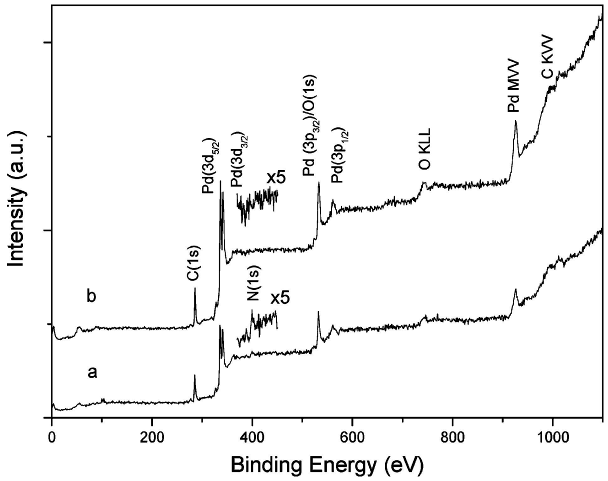

Figure 4 XPS survey spectra of Pd nanoparticles: (a) EA-produced and (b) EtOH-produced. Inset is high-resolution N_{1s} core level XPS spectra.

particles sticky onto the magnetic stirring bar, no major change was observed even after 2 months. Enhanced solubility of $Pd(OAc)_2$ in EA aqueous solution (note: $Pd(OAc)_2$ is insoluble in water) is due to the $NH_2 \rightarrow Pd$ interaction. The decrease in reducibility of EA aqueous solution is due to strong hydrogen bond between -OH groups in EA and water (exothermic when mixing EA and water). It indicates the reducibility of EA originates from its -OH group, as stated in the literature [8–10].

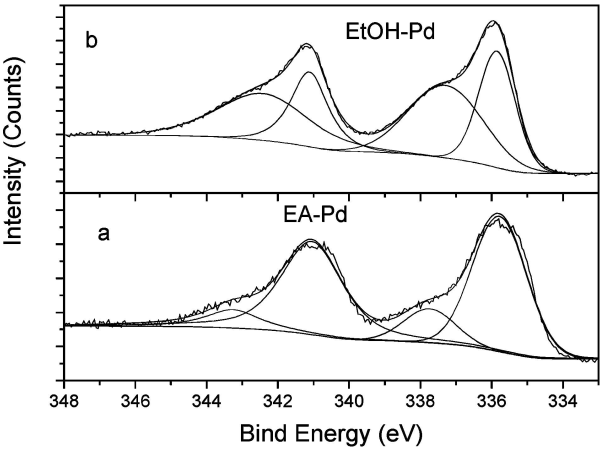

Figure 5 Pd_{3d} core level XPS spectra of Pd nanoparticles: (a) EA-produced and (b) EtOH-produced.

Acknowledgment

FX Chen acknowledged the financial support by ICES in-house project (project code: ICES/03-112002).

References

1. J. C. LOVE, D. B. WOLFE, R. HAASCH, M. L. CHABINYC, K. E. PAUL, G. M. WHITESIDES and R. G. NUZZO, *J. Amer. Chem. Soc.* **125** (2003) 2597.
2. M. CROCKER, J. G. BUGLASS and R. H. M. HEROLD, *Chem. Mater.* **5** (1993) 105.
3. A. BECK, A. HORVÁTH, A. SZÜCS, Z. SCHAY, Z. E. HORVÁTH, Z. ZSOLDOS, I. DÉKÁNY and L. GUCZI, *Catal. Lett.* **65** (2000) 33; A. HORVÁTH, A. BECK, A. SÁRKÁNY and L. GUCZI, *Solid State Ionics* **148** (2002) 219.
4. S. PUVVADA, S. BARAL, G. M. CHOW, S. B. QADRI and B. R. RATNA, *J. Amer. Chem. Soc.* **116** (1994) 2135.
5. S. AYYAPAN, R. S. GOPALAN, G. N. SUBBANA and C. N. R. RAO, *J. Mater. Res.* **12** (1997) 398.
6. S. OKEYA, H. SAZAKI, M. OGIKA, T. TAKEMOTO, Y. ONUKI, Y. NAKAMURA, B. K. MOHAPATRA and S. KAWAGUCHI, *Bull. Chem. Soc. Jpn.* **54** (1981) 1978.
7. M. R. MUCALO and C. R. BULLEN, *J. Mater. Sci. Lett.* **20** (2001) 1853.
8. W. LU, B. WANG, K. WANG, X. WANG and J. G. HOU, *Langmuir* **19** (2003) 5887.
9. N. TOSHIMA, *J. Macromol. Sci. Chem.* A **27** (1990) 1225.
10. M. TOSHIMA, T. YONAZAWA and K. KUSHIHASHI, *J. Chem. Soc., Faraday Trans.* **89** (1993) 2537.

Received 7 April
and accepted 27 July 2004